Root angle modifications by the *DRO1* homolog improve rice yields in saline paddy fields

Yuka Kitomi[a], Eiko Hanzawa[b], Noriyuki Kuya[a], Haruhiko Inoue[c,d], Naho Hara[c], Sawako Kawai[a,1], Noriko Kanno[a], Masaki Endo[c], Kazuhiko Sugimoto[a], Toshimasa Yamazaki[e], Shingo Sakamoto[f], Naoki Sentoku[c], Jianzhong Wu[a], Hitoshi Kanno[g], Nobutaka Mitsuda[f], Kinya Toriyama[g], Tadashi Sato[g,2,3], and Yusaku Uga[a,2,3]

[a]Institute of Crop Science, National Agriculture and Food Research Organization (NARO), 305-8518 Tsukuba, Ibaraki, Japan; [b]Graduate School of Life Sciences, Tohoku University, 980-8577 Sendai, Miyagi, Japan; [c]Institute of Agrobiological Sciences, NARO, 305-8634 Tsukuba, Ibaraki, Japan; [d]PRESTO, Japan Science and Technology Agency (JST), 332-0012 Kawaguchi, Saitama, Japan; [e]Advanced Analysis Center, NARO, 305-8517 Tsukuba, Ibaraki, Japan; [f]Bioproduction Research Institute, National Institute of Advanced Industrial Science and Technology (AIST), 305-8566 Tsukuba, Ibaraki, Japan; and [g]Graduate School of Agricultural Science, Tohoku University, 980-8572 Sendai, Miyagi, Japan

The root system architecture (RSA) of crops can affect their production, particularly in abiotic stress conditions, such as with drought, waterlogging, and salinity. Salinity is a growing problem worldwide that negatively impacts on crop productivity, and it is believed that yields could be improved if RSAs that enabled plants to avoid saline conditions were identified. Here, we have demonstrated, through the cloning and characterization of *qSOR1* (*quantitative trait locus for SOIL SURFACE ROOTING 1*), that a shallower root growth angle (RGA) could enhance rice yields in saline paddies. *qSOR1* is negatively regulated by auxin, predominantly expressed in root columella cells, and involved in the gravitropic responses of roots. *qSOR1* was found to be a homolog of *DRO1* (*DEEPER ROOTING 1*), which is known to control RGA. CRISPR-Cas9 assays revealed that other *DRO1* homologs were also involved in RGA. Introgression lines with combinations of gain-of-function and loss-of-function alleles in *qSOR1* and *DRO1* demonstrated four different RSAs (ultra-shallow, shallow, intermediate, and deep rooting), suggesting that natural alleles of the *DRO1* homologs could be utilized to control RSA variations in rice. In saline paddies, near-isogenic lines carrying the *qSOR1* loss-of-function allele had soil-surface roots (SOR) that enabled rice to avoid the reducing stresses of saline soils, resulting in increased yields compared to the parental cultivars without SOR. Our findings suggest that *DRO1* homologs are valuable targets for RSA breeding and could lead to improved rice production in environments characterized by abiotic stress.

abiotic stress | gravitropism | *Oryza sativa* L. | quantitative trait locus (QTL) | root trait

Optimized plant architecture, both above and below ground, is required for plants to adapt to different environments (1, 2). The optimization of plant architecture has also been one of the most effective ways to improve crop productivity. The "Green Revolution," which began in the 1950s, resulted in new, high-yielding varieties of wheat and rice due to the introduction of dwarfing genes into traditional, tall varieties: *Reduced height* (*Rht*) in wheat and *semidwarf1* (*sd1*) in rice (3). In rice, several additional genes associated with its above-ground architecture, such as *Tiller Angle Control 1* (*TAC1*), which controls tiller angle, and *Ideal Plant Architecture 1* (*IPA1*), which regulates tiller number (4–6), have also been identified. Root system architecture (RSA), however, has not experienced the same level of improvement due to the difficult nature of phenotyping the below-ground part of the plants and the limited genetic information available to breeders. Nonetheless, RSA is recognized as an important trait that, if understood, could be improved to allow plants to adapt to a range of soil environments, such as those experiencing deficiencies or excesses of water and/or nutrients (7, 8). Typically, a deep RSA is beneficial for enhancing drought avoidance, whereas a shallow RSA facilitates the acquisition of

phosphorus (P) in P-deficient soils. Another unique root system is soil-surface roots (SOR), which may enable upland plants to adapt to waterlogging, by allowing them to obtain oxygen from the air (9). Thus, an improved understanding of the factors controlling RSA could enable the breeding of crop cultivars that are suitable to the different stress conditions caused by global climate change (10).

Many rice genes involved in root development have already been isolated (11). *LARGE ROOT ANGLE1* encoding *OsPIN2* and *DEFECTIVE IN OUTER CELL LAYER SPECIFICATION 1* (*DOCS1*) belonging to the leucine-rich repeat receptor-like kinase (LRR-RLK) subfamily, control gravitropic responses (12, 13). *Rice Morphology Determinant* (*RMD*), encoding an actin-binding protein, controls gravitropic responses to low external phosphate conditions (14). These genes affect the root growth angle (RGA) and determine RSAs in rice. However, only a limited number of previously identified RSA-controlling genes have promise, for the breeding of future climate-resilient rice (15). One of these candidates is *DEEPER ROOTING 1* (*DRO1*), a quantitative trait locus (QTL) that has previously been cloned and shown to affect vertical root distributions in the soil (16). The deeper rooting habit conditioned by the functional allele at *DRO1* enhanced grain yields under drought stress, while the

Significance

Genetically improving the root system architectures of plants is an effective strategy for developing climate-resilient crops. In this study, we revealed that a cloned rice quantitative trait locus associated with root growth angle, *qSOR1*, is a *DRO1* homolog involved in root gravitropic responses. The loss-of-function allele *qsor1* resulted in roots that developed on the soil surface and enabled plants to avoid the reducing stress found in saline paddy soils and, consequently, increased yields. We show that the *DRO1* homologs could be useful for the controlled breeding of root system architectures that are adapted to the abiotic stress conditions caused by global climate change.

shallow rooting allele, *dro1,* was associated with drought susceptibility. To develop rice cultivars that are robust to environmental stress conditions other than drought, it is necessary to identify and characterize additional QTLs associated with variations in the RSA-related attributes.

Rice cultivars ordinarily develop underground crown roots. We previously identified SOR phenotypes in Gemdjah Beton (GB), an Indonesian lowland rice belonging to the Bulu ecotype (17). SOR may occur due to the selection pressures within Bulu cultivars to adapt to severe anaerobic environments (18). We previously fine-mapped a QTL for *SOIL SURFACE ROOTING 1,* *qSOR1* on rice chromosome 7, using mapping populations derived from a cross between GB and a non-SOR lowland rice cultivar called Sasanishiki (SA) (19). Previously, a gene related to the SOR phenotype, *SOR1,* was identified on rice chromosome 4 using a mutant line (20). SOR1 has a function like *Arabidopsis WAV3,* which is an E3 ubiquitin ligase that controls root gravitropism by affecting auxin responses (21, 22). The *qSOR1* locus identified in this study maps to a different region (chr 7), and since no *SOR1* homologs were found in the candidate region of the *qSOR1* locus,

it was concluded that *qSOR1* may have a different function from that of *SOR1.*

Here, we report that the functional gene, *qSOR1,* is a *DRO1* homolog involved in gravitropic responses that acts through negative regulation via auxin signaling. Furthermore, we demonstrate that the SOR phenotype originates from a loss-of-function of *qSOR1* and contributes to the avoidance of the reducing stress conditions in saline paddies, leading to yield enhancement. Our results suggest that the natural alleles of *DRO1* homologs will be useful for the genetic improvement of the RSA of rice.

Results

Phenotypic Characteristics and Map-Based Cloning of *qSOR1.* To elucidate the effects of *qSOR1* on root morphology, we developed a near-isogenic line (NIL), homozygous for the GB allele of *qSOR1* in a SA background (qsor1-NIL) (Fig. 1*A*). The qsor1-NIL readily developed SOR that resembled those of the GB cultivar, whereas the SA cultivar developed relatively fewer SOR (*SI Appendix,* Fig. S1 *A–C*). The qsor1-NIL showed markedly shallower RGA than the SA (Fig. 1 *B–D*), but there were no differences in the other
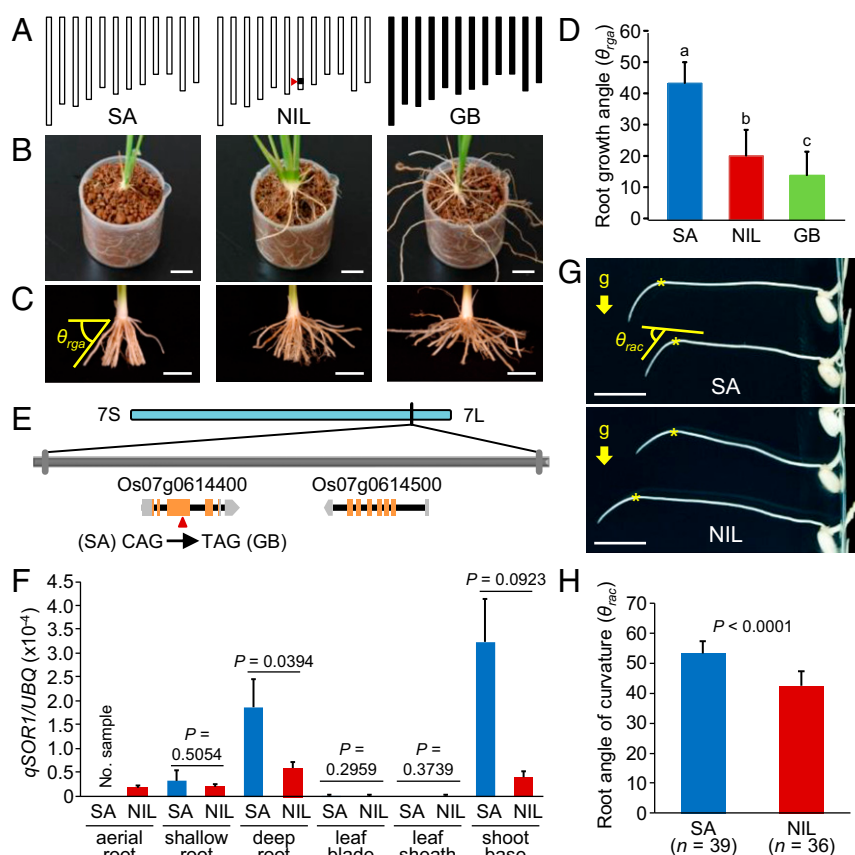
Fig. 1. Phenotypic and molecular characterization of *qSOR1.* (*A*) Graphical genotypes of Sasanishiki (SA; *Left*), qsor1-NIL (NIL; *Center*), and Gemdjah Beton (GB; *Right*). The white and black rectangles indicate the homozygous regions from SA and GB, respectively. Red arrowhead, position of *qSOR1.* (*B*) Images of rice plants grown in small cups for 20 d after sowing and after the removal of the topsoil from each cup. (*C*) Images of the basal parts of the rice plants grown in the cups in *B*. The root growth angle (θ_{rga}) of each plant was determined by measuring the angle between the horizontal line and the shallowest nodal root. (*D*) Mean root growth angle of SA, qsor1-NIL, and GB. Data are means + SD; $n = 40$, 38, and 36 plants for SA, qsor1-NIL, and GB, respectively. Different letters indicate significant differences ($P < 0.01$, Tukey's HSD test). (*E*) Sequence variations between SA and GB in the two putative ORFs detected in the candidate region of the *qSOR1* locus. Red arrowhead, a single 1-bp substitution. Orange rectangles, ORF; gray rectangles, 5′ and 3′ UTRs. (*F*) *qSOR1* expression in various shoot and root tissues. Samples of the root tips from different depths, leaf blades, leaf sheaths, and shoot bases (1-cm sample from the bottom of the shoot) were taken from plants grown in baskets, 30 d after sowing. Expression of *qSOR1* was normalized to that of rice *Ubiquitin* gene. Data are shown as mean + SD; $n = 3$ biological repeats. *P* values are based on Student's *t* tests. (*G*) Gravitropic curvature in the seminal roots of SA and qsor1-NIL plants. θ_{rac} is the root angle of the curvature after rotation. Asterisks indicate the positions of the root tips at the start of the rotation. Yellow arrows indicate the direction of the gravitational force. (*H*) Root angle of the curvature of SA and qsor1-NIL after rotating 90° from the original vertical axis for 4 h. *P* value is based on Student's *t* test. (Scale bars: 1 cm.)

root and shoot morphologies (*SI Appendix*, Fig. S1*D*). These results indicate that *qSOR1* predominantly controls RGA.

To isolate the *qSOR1* gene, we identified a candidate region within a 12.31-kb segment using positional cloning (*SI Appendix*, Fig. S2). Comparing the genomic sequences of the candidate region between GB and SA, a single 1-bp substitution within exon 3 of one of the putative ORFs (Os07g0614400; LOC_Os07g42290.1) was identified. The GB allele at this ORF coded for an unknown protein, and the 1-bp mutation resulted in a premature stop codon (Fig. 1*E* and *SI Appendix*, Fig. S3*A*). Three-dimensional modeling of the qSOR1 candidate protein showed that the premature stop truncated a polypeptide in GB, which inhibited the formation of the helix bundle structure due to a lack of helix–helix interactions (*SI Appendix*, Fig. S3 *B–D*). Haplotype analysis for this ORF revealed that the Bulu cultivars with SOR phenotypes commonly possessed this 1-bp substitution, but other accessions that lacked SOR did not (*SI Appendix*, Table S1). Transgenic plants that carried a 7.57-kb genomic DNA fragment from SA, containing the entire Os07g0614400 ORF in the qsor1-NIL (gSA/NIL) genetic background, showed increased RGAs compared to those transformed with an empty vector (Vec/NIL) (*SI Appendix*, Figs. S2*B* and S4 *A* and *B*). Therefore, we concluded that the SOR phenotype observed in the GB was caused by the loss-of-function mutation in exon 3 of Os07g0614400.

Root Gravitropic Responses Mediated by *qSOR1* Are Controlled by Auxin Signaling. *qSOR1* was mainly expressed in the tips of deeper roots, the shoot base with crown root primordia, and the floral organs, whereas *qSOR1* mRNA was hardly detected in the leaf blade or the sheath (Fig. 1*F* and *SI Appendix*, Fig. S5*A*). Although *qSOR1* had its highest expression levels in the floral organs, their sizes in the SA cultivar and in the qsor1-NILs were comparable, indicating that the loss of function of *qSOR1* (*qsor1*) had few effects on floral morphology (*SI Appendix*, Fig. S5*B*). The root tip is the main organ involved in gravitropic sensing, which determines the direction of root elongation (23), and we employed in situ hybridization to observe the spatial expression of *qSOR1* within it. Signals were mainly detected in and around the gravity-sensing columella cells, called statocytes (23), and the expression patterns in SA, qsor1-NIL, and GB were equivalent (*SI Appendix*, Fig. S6*A*). The SA roots responded more sharply to rotations from a normal vertical to a horizontal axis than did those of the qsor1-NIL (Fig. 1 *G* and *H*). Roots of gSA/NIL also showed sharper gravitropic responses than did those of Vec/NIL (*SI Appendix*, Fig. S4 *C* and *D*). The *qSOR1* expression pattern was stable even if the gravitational vector was changed (*SI Appendix*, Fig. S6*B*). To investigate whether the *qSOR1* was involved in the development of statocytes, we stained amyloplasts in the columella cells of seminal roots. We found that the starch accumulation was indistinguishable between the SA and qsor1-NIL plants (*SI Appendix*, Fig. S7*A*). The size and number of the columella cells in the crown roots was also identical between the SA and qsor1-NIL (*SI Appendix*, Fig. S7 *B–F*). These findings suggested that the altered gravitropic response in the qsor1-NIL was not due to changes in the spatial expression patterns of *qSOR1* or to morphological changes in the root columella cells.

We conducted qRT-PCR to monitor auxin responses in SA and the qsor1-NIL, as the phytohormone auxin plays a key role in root gravitropism. *qSOR1* expression in both lines declined within 30 min of the application of the exogenous auxin (*SI Appendix*, Fig. S8*A*). We also examined the effects of the protein synthesis inhibitor cycloheximide (CHX) on seedlings with the auxin-dependent reduction of *qSOR1* but found that it was not inhibited (*SI Appendix*, Fig. S8*B*), suggesting that de novo protein synthesis was not required for *qSOR1* reduction by auxin. In the *qSOR1* promoter region, we found two auxin response elements (AuxREs) (*SI Appendix*, Fig. S8*C*), corresponding to the TGTCTC motif for the ARF protein to bind to, to regulate the transcription of early auxin response genes (24, 25). This

indicated that *qSOR1* may be an early auxin response gene directly regulated by the auxin signaling pathway.

Rice *DRO1* Homologs Affect RGA. When qSOR was compared to all protein sequences in rice, it was found to be most closely related to DRO1 (*SI Appendix*, Fig. S3*A*). Recently, homologs of rice *DRO1* and *LAZY,* which has sequence similarities with *DRO1*, have been shown to be involved in the gravitropism of shoots or roots in several plants (26–29). Phylogenic analysis of the *DRO1* gene family in monocots and dicots revealed that many dicots had more similar sequences to *qSOR1* (*DRO1-like 1, DRL1*) than to *DRO1* (Fig. 2*A* and *SI Appendix*, Table S2). This suggests that the *qSOR1* sequence may be more universal than the *DRO1* in angiosperms. Phylogenic analysis also showed that additional *DRO1* homologs (*DRO1-like 2, DRL2*) were found in rice, maize, and sorghum (Fig. 2*A*). To determine whether *DRL2* regulates RGA in rice, knockout lines of *DRL2* were created using the clustered regularly interspaced short palindromic repeat (CRISPR)/ CRISPR-associated protein 9 (Cas9) system (*SI Appendix*, Fig. S9). The knockout lines displayed smaller RGAs than the WT plants, like the *qSOR1* and *DRO1* knockout lines (Fig. 2 *B* and *C*), but with weaker gravitropic responses than the *qSOR1* and *DRO1* lines (*SI Appendix*, Fig. S10). *DRL2* is located near the same chromosome region as the rice QTLs for RGA (19, 30), suggesting that there may be natural *DRL2* variants in rice. Thus, the *DRO1* family, consisting of three subgroups, plays a critical role in the genetic variation of RGA in rice.

Conserved C-Terminal among the *DRO1* Homologs Is Indispensable for RGA Control. A region at the C-terminal of *DRO1* homologs, which includes the WxxTD and EAR-like motifs, is well conserved, despite the relatively low homology of the proteins (*SI Appendix*, Fig. S3*A* and refs. 28 and 31). Recently, the role of this domain has been revealed in *Arabidopsis*. Taniguchi et al. designated the domain, including 14 critical amino acid sequences, as the conserved C terminus in the LAZY1 family of proteins (CCL) and demonstrated that the CCL domains in the *qSOR1*/ *LAZY* homologs of *Arabidopsis* were required for RGA control (28, 29). The interactions between the CCL domains of the *LAZY1-LIKE* (*LZY*) and the Brevis radix (BRX) domains of the RCC-like domain (RLD) proteins that regulate polar auxin transport are important processes that determine gravitropic responses in *Arabidopsis* root systems (32). To examine the function of this conserved region in rice, we made a series of transgenic constructs consisting of the 3.4-kb *qSOR1* native promoter and truncated *qSOR1* cDNA sequences (*SI Appendix*, Fig. S11*A*). Deletion lines introducing *qSOR1* complimentary DNA (cDNA) without the N-terminal sequences showed similar RGAs to the positive control line, harboring the full-length *qSOR1* cDNA from SA (*SI Appendix*, Fig. S11*B*). Deletion lines harboring the *qSOR1* cDNA without the C-terminal sequences showed shallow RGA phenotypes, like the Vec/NIL. These results suggest that the conserved regions in the C-terminal of the *DRO1* homologs are essential for RGA control in both dicots and monocots.

Like *DRO1* (16), *qSOR1* was involved in gravitropic responses under auxin signaling. However, *qSOR1* was mainly expressed around columella cells, while *DRO1* was expressed in the whole root meristems, except for the columella cells. To determine the subcellular localization of the qSOR1 proteins, we introduced a construct encoding an EGFP-fusion protein of the full-length qSOR1 from SA and that of a truncated qSOR1 from GB into rice protoplasts. EGFP fluorescence was observed in the plasma membrane for the full-length qSOR1 constructs (*SI Appendix*, Fig. S12). In contrast, the truncated qSOR1 protein without the conserved C-terminal, which was pivotal for RGA control, was not localized to the plasma membrane. These results indicated that the conserved C-terminal was needed for both protein
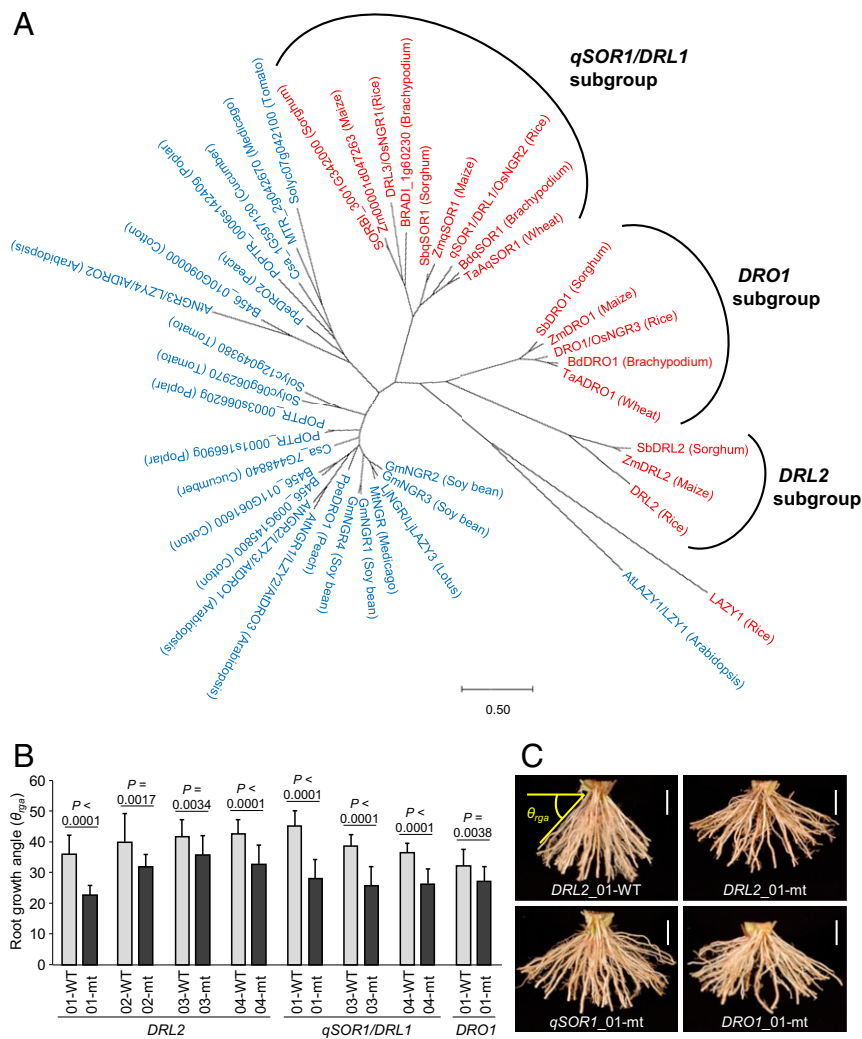
Fig. 2. Effects of *DRO1* homologs on root growth angle. (*A*) Phylogenic tree of full-length protein sequences sharing similarities with DRO1 and qSOR1 from both monocots and dicots. The gene names in red and blue are monocots and dicots, respectively. Scale bar shows distance estimated from amino acid substitutions. Correspondences between gene names in the tree and gene IDs are shown in *SI Appendix*, Table S2. (*B*) Root growth angle (θ_{rga}) of the CRISPR-Cas9 lines. The RGA of the plants grown in stainless-steel mesh baskets for 6 wk after sowing was determined by measuring the angle between the horizontal line and the shallowest nodal root. mt, homozygous mutant allele in target gene; WT, homozygous null allele in target gene. Data are shown as mean + SD. *P* values are based on the Student's *t* tests. (*C*) Images of the basal parts of the rice plants grown in the basket described in *B*. (Scale bars: 1 cm.)

function and the subcellular localization of qSOR1. Similar observations were previously found in rice DRO1 (16). These findings suggest that the two genes may have similar functions for RGA control in differently expressed tissues, although further analysis will be needed to clarify the role of each gene with regard to root gravitropic responses.

Natural Alleles of the *DRO1* Homologs Contribute to RSA Variations in Rice. To clarify the how *qSOR1* and *DRO1* regulate RGA, we used IR64, lowland rice, and three introgression lines (ILs) carrying *DRO1* and *qSOR1* alleles in an IR64 background (Fig. 3*A*). When comparing the *DRO1* expression between the *qSOR1* and *qsor1* backgrounds, and the *qSOR1* expression between the *DRO1* and *dro1* backgrounds, respectively, no marked differences were found (*SI Appendix*, Fig. S13 *A* and *B*). The amyloplast and columella cell development were also identical among the four lines (*SI Appendix*, Fig. S7). The RGA assay discovered differences in RGA, resulting in deep to shallow rooting in the order of the lines of [*DRO1*, *qSOR1*], [*DRO1*, *qsor1*], [*dro1*, *qSOR1*], and [*dro1*, *qsor1*], indicating that *DRO1* and *qSOR1* act additively to determine RGA

(*SI Appendix*, Fig. S13 *C* and *D*). We also measured the tiller angles of the four lines because *LAZY1*, which is a gene in the *LAZY* family, is associated with tiller angle in rice (33). These lines had no significant differences in tiller angle (*SI Appendix*, Fig. S13E). The expression and phenotypic assays suggested that *qSOR1* functions in a distinct pathway from the *DRO1* to determine RGA, and that neither gene contributes to tiller angle.

The RGA differences in the four lines observed using the basket assay were confirmed in the upland environment (Fig. 3 *B–D*), although the [*dro1*, *qsor1*] line showed an extremely small shoot biomass compared to the other three lines (*SI Appendix*, Fig. S14A). There was little difference between the shoot morphologies of the lines grown in the paddy (*SI Appendix*, Fig. S14B). The suppressed phenotype in the [*dro1*, *qsor1*] line grown in the upland environment may be due to the extremely small root zone that resulted in reduced acquisition of water and nutrients from the soil. These results indicated that RGA alterations conditioned by *dro1* and *qsor1* had little impact on plant growth if the plants had access to adequate water and nutrients, as they did in the paddy environment.
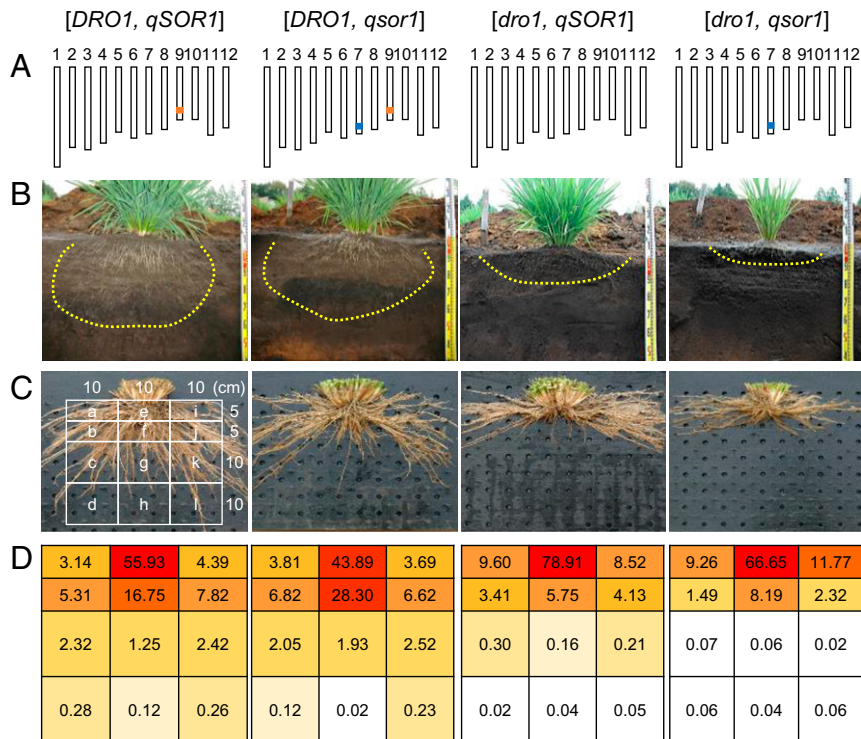
Fig. 3. Effects of the genetic interactions of *qSOR1* and *DRO1* on the root system architecture in upland conditions. (*A*) Graphical genotypes of the four lines investigated; [*DRO1*, *qSOR1*], [*DRO1*, *qsor1*], [*dro1*, *qSOR1*], and [*dro1*, *qsor1*] in the IR64 background. White rectangles indicate homozygous alleles of IR64. Orange boxes and blue boxes indicate segments of homozygous alleles of Kinandang Patong, including functional alleles of *DRO1* and of the GB including nonfunctional alleles of *qSOR1*, respectively. IR64 originally had a nonfunctional allele of *DRO1* and a functional allele of *qSOR1*. (*B*) Root distributions of 4-mo-old rice plants assessed using the trench method. Yellow dashed lines indicate the extent of the root elongation. (*C*) Typical root distributions of each line obtained using the monolith sampler. (*D*) Heatmap showing the ratio of the root distributions in each monolith block. Each soil monolith was divided into 12 blocks (a to l in *C*), and the root dry weight in each block was measured and the root distribution ratio calculated. Data are means + SD; *n* = 10 (5 plants × 2 repeats).

Rice with SOR Can Avoid Reducing Stresses in Saline Paddy Soils.

Saltwater incursions into paddy fields result in increased salt concentrations in the soil (Fig. 4*A*). We hypothesized that the SOR trait allowed rice roots to avoid the salt that settled in the soil. In the paddy fields, the qsor1-NIL had more SOR than the SA, irrespective of the saline-water treatment (*SI Appendix*, Fig. S15 *A* and *B*). Salinity promotes shallower RGA of *Arabidopsis* by weakening the gravitropic response (34). Using seedlings grown in agarose media with NaCl, we found that the gravitropic response was weakened by the salinity stress in the rice roots as well, irrespective of the genetic backgrounds of the functional or nonfunctional alleles at *qSOR1* (*SI Appendix*, Fig. S16). These results suggest that salinity stress is not directly involved in SOR formation. We then investigated the effects of SOR on grain yields in conditions of saline stress. In the saline paddies, the qsor1-NIL had well-conditioned leaves through maturity and better grain filling than the SA (Fig. 4*B* and *SI Appendix*, Fig. S15 *C* and *D*), resulting in increased yields of more than 15%, compared to average SA yields over 4 y (Fig. 4*C*), although both lines showed similar shoot morphologies (*SI Appendix*, Table S3). The Na⁺ concentrations in the xylem exudates were identical for both lines under salinity stress, suggesting that the observed differences in RSA did not affect Na⁺ uptake (*SI Appendix*, Fig. S15*E*). Soil reduction assays showed that saline soils tended to be reduced compared to normal soils (Fig. 4*D* and *SI Appendix*, Fig. S15*F*). We concluded that SOR may help rice avoid reducing stresses in saline paddy soils, although further analysis is required to better understand the utility of this approach.

Discussion

The SOR phenotype has been reported in cultivated rice and in wild relatives of maize (teosinte) (9, 17). Previously, QTL mapping was conducted to elucidate and utilize the natural variation for SOR in these plants (19, 35, 36), but the gene(s) underlying the SOR QTLs had not been isolated. In this study, we cloned a rice QTL related to SOR using map-based cloning. Phylogenic analysis found that the *qSOR1* gene is a *DRO1* homolog in rice (Fig. 2*A*). We also revealed that, like *DRO1*, *qSOR1* is negatively regulated by auxin signaling and involved in gravitropism (*SI Appendix*, Fig. S8 and Fig. 1 *G* and *H*). Gene expression studies and phenotypic analyses for RGA using *qSOR1* and *DRO1* introgression lines showed that both genes independently controlled RGA (*SI Appendix*, Fig. S13 *A–D*). Compared with the [*DRO1*, *qSOR1*] line, the [*dro1*, *qSOR1*] line had shallower whole root systems, whereas the [*DRO1*, *qsor1*] line had both shallow and deep roots. The differences in the RSA phenotypes of the lines with loss-of-function alleles for *DRO1* or *qSOR1* may be related to differences in their tissue-specific expression patterns of the two genes. Genes belonging to the *LAZY* family, including *qSOR1* and *DRO1*, have been identified in both monocots and dicots (28, 37). These genes are classified into three types: those that affect only shoot gravitropism, only root gravitropism, and those that affect the gravitropism of both organs (37). Our results show that *qSOR1* and *DRO1* are involved only in root gravitropism, but they have different roles in the process, suggesting that multiple *DRO1* homologs contribute to the genetic variation of RGA in rice. The fact that *DRL2* was shown to control RGA further supports this hypothesis. To apply *DRO1*
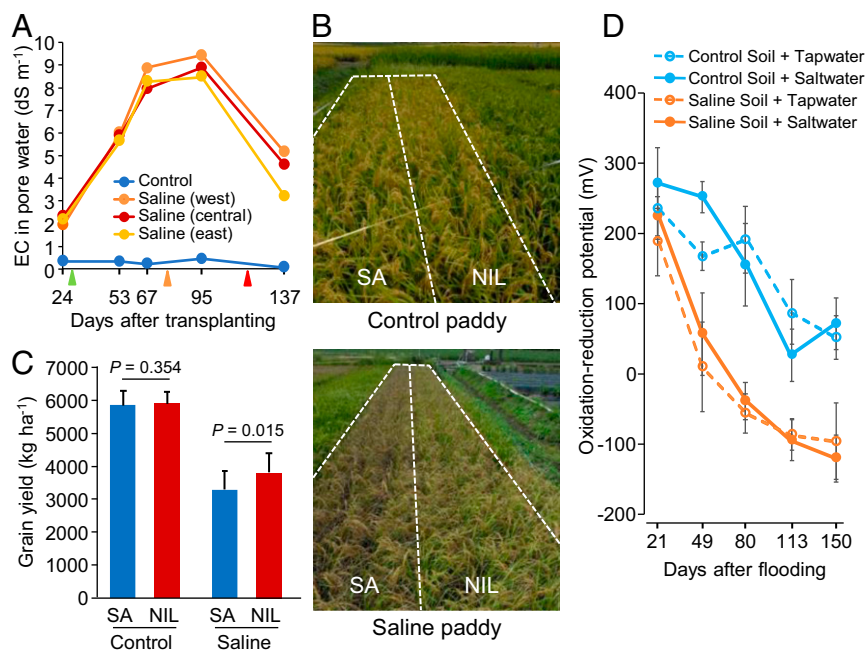
Fig. 4. Effects of *qsor1* soil-surface roots on grain yields in saline paddies. (*A*) Temporal changes of the EC values of the pore water in the paddy soils (at depths of 5–10 cm) with or without saline-water treatments in 2016. Green, orange, and red arrowheads indicate the time points when saline-water treatments started, the heading date, and harvest date, respectively. Control, paddy with fresh water; Saline, paddy with saline water (about 0.4%). West, central, and east indicate the west, central, and east sides of the paddy field, respectively. (*B*) Side views of the typical rice conditions with fresh or saline water at the stage of maturity. In the saline conditions, the qsor1-NIL plants had leaves that were considerably greener, in comparison with the SA plants. (*C*) Average grain yields in the SA and qsor1-NIL, grown in the control and saline paddies (crude brown rice). Data are means + SD; *n* = 14 replicate plots over 4 trial years (2015–2018). *P* values are based on ANOVA. (*D*) Oxidation-reduction potentials in the saline and normal paddy soils after flooding treatments with or without saline water. Data are shown as mean ± SD; *n* = 6 soil samples (3 plots per year × 2 y).

homologs efficiently in molecular breeding for RSA, it is necessary to clarify in detail, the different functions of each gene.

Yield trials using SA and qsor1-NIL over 4 y demonstrated that SOR contributed to improved yields in saline paddies, although the presence or absence of SOR did not affect the yield performance between SA and qsor1-NIL in the control paddies. We initially anticipated that SOR would enable the rice root system to avoid soil with high-salt concentrations in saline paddies. However, SOR did not affect salt absorption (*SI Appendix*, Fig. S15*E*). Soil reduction, however, was observed in our experimental paddy fields that were treated with saline water for more than 20 y. The accumulation of excess Na^+ in the soil generally results in undesirable soil structures, like increased soil bulk density. These soil structures have adverse effects on other soil physical properties, such as aeration and drainage performance (38), resulting in increased soil reduction. Such soil physical properties in saline paddies cause rice root development to be stunted (39). We also know, from previous studies, that saline soils create toxic reduced environments, similar to those created by Fe, Al, and organic acids (40). Consequently, it is presumed that SOR help plants to avoid reducing conditions, rather than directly avoiding the salinity stress, however, further investigations on the physiological benefits of SOR in saline paddies are needed.

SOR is one of the most reliable adaptations of upland crops to avoid waterlogging, since it enables the roots to obtain oxygen from the air (9, 41). To improve the tolerance to waterlogging, SOR and adventitious root formation under hypoxic environments have been studied in maize and soybean (42, 43). In rice, SOR is specifically found in the Bulu ecotype, which is grown in severe anaerobic conditions (18). Even in rice, which is a marsh plant, excessively reduced soils decrease yields, as the roots are damaged by mineral toxicities (44, 45). Therefore, the Bulu

ecotype may have used SOR to avoid such anaerobic conditions. Our haplotype analysis showed that only Bulu cultivars from Indonesia with SOR carried the loss-of-function allele at *qSOR1* (*SI Appendix*, Table S1). Natural populations of *Arabidopsis* grown in high-latitude regions (i.e., north of Sweden) are known to carry a specific allele of *CYTOKININ OXIDASE 2* (*CKX2*) that produces a shallower RGA; this allele may confer a selective advantage allowing plants to adapt to soil hypoxia caused by snow and thaw (46). For a similar reason, the loss-of-function allele of *qSOR1* may confer a selective advantage in Bulu cultivars grown in severe anaerobic conditions.

Since salinity is a major abiotic stress that is expected to impact negatively on an estimated 50% of all arable soils worldwide by 2050 (47), our work suggests that global food production could be improved by selecting for RSAs that can avoid the damage caused by saline conditions (10). Saltwater intrusions and waterlogging in coastal regions due to sea level rise and cyclones, which will be exacerbated by climate change, threaten crop productivity worldwide (48). In the case of paddy rice, which is a staple food in those swampy regions, *qsor1* could prove to be a valuable breeding target to improve yields in saline paddy fields. The allele is globally rare, but locally common; the only rice cultivars known to carry this allele are Bulu ecotypes from Indonesia. In addition to saline paddy fields, SOR may be effective at avoiding damage caused by other stresses that result from reduced paddy conditions, such as excess iron. Moreover, as shallow rooting is known to be advantageous for P uptake in P-deficient soils (7), SOR may be beneficial for rice in P-deficient paddies. To clarify the relationship between SOR and nutrient uptake, further investigations are required. Our results also suggest that the *qSOR1* homologs may help other upland crops such as maize and soybean to avoid waterlogging, as they were found in many other terrestrial plants.

qSOR1 and *DRO1* function independently to determine RGA and have few adverse effects on shoot morphologies, making them useful for RSA breeding. *TAC1* homologs, which share conserved motifs with the *DRO1* homologs (but not the C-terminal EAR-like motif), determine shoot growth angle in several species (4, 49, 50). *TAC1* has been utilized in rice breeding to make shoot architecture more efficient and to increase photosynthetic efficiency in dense planting regimes (4). *DRO1* homologs could become powerful driving forces of the "Second Green Revolution" by improving root growth angles to enable plants to avoid a variety of environmental stresses, including drought, waterlogging, and saltwater intrusions.

Materials and Methods

Plant Materials. GB is a traditional *japonica* lowland rice cultivar (ecotype Bulu) that originated in Indonesia and grows crown roots on the soil surface. SA is a modern *japonica* lowland rice cultivar released in Japan that does not grow soil-surface roots. To characterize *qSOR1*, we developed a near-isogenic line, homozygous for the GB allele of *qSOR1* (qsor1-NIL: BC_3F_3) by repeated backcrossing with SA, and DNA marker-assisted selection to eliminate the nontarget chromosomal regions. To elucidate the relationships that *qSOR1* and *DRO1* have with RGA regulation, we prepared four lines with differing combinations of the functional and nonfunctional alleles for *qSOR1* and *DRO1* in the genetic background of the *indica* lowland rice variety, IR64: [*DRO1*, *qSOR1*], [*DRO1*, *qsor1*], [*dro1*, *qSOR1*], and [*dro1*, *qsor1*]. IR64 has a nonfunctional allele of *DRO1* (*dro1*) and a functional allele of *qSOR1*. We used Dro1-NIL, developed in a previous study (16), for [*DRO1*, *qSOR1*]. We selected a line [*dro1*, *qsor1*] from the BC_4F_4 advanced-backcross progeny, derived from a cross between IR64 (recurrent parent) and GB (donor parent). To develop [*DRO1*, *qsor1*], we crossed the BC_2F_1 advanced-backcross progeny of IR64 × GB with the Dro1-NIL, and selected a BC_4F_5 line with [*DRO1*, *qsor1*].

Quantification of Soil-Surface Roots, RGA, and Other Root Traits. To measure the number of soil-surface roots, 30 open stainless-steel mesh baskets (7.5 cm diameter × 5.0 cm depth) were buried just under the soil surface, in soil-filled plastic containers (68 × 42 × 16 cm). One germinated seed was placed at the center of each soil-filled basket. From the second leaf stage, the water level in each plastic container was maintained at the soil surface level with tap water. The plants were grown in the greenhouse at 30 °C under natural daylight. Six weeks after sowing, we counted the number of primary roots growing over the open sides of the baskets. To measure RGA, the rice plants were grown in plastic cups or stainless-steel mesh baskets as described previously (16, 19). After washing the roots in each basket, the RGA of each plant was determined by measuring the angle between the soil surface (horizontal line) and the shallowest primary root, with a protractor. The maximum root length, crown root number, and root dry weight of SA and the qsor1-NIL grown in the hydroponic system were measured, as described previously (51).

High-Resolution Mapping of *qSOR1*. We previously mapped *qSOR1* between the simple sequence repeat (SSR) markers RM21941 and RM21976 (19) (*SI Appendix*, Fig. S2*B*). For the high-resolution mapping of *qSOR1* in this study, we selected recombinant homozygous lines from an advanced-backcross progeny derived from a cross between SA (recurrent parent) and one recombinant inbred line (GS34), in which the target QTL region was homozygous for the GB (donor parent) allele. We developed 4,806 BC_3F_2 plants by selfing the BC_3F_1 plants that were heterozygous for the *qSOR1* region. We selected BC_3F_2 plants in which recombination had occurred within the region containing *qSOR1*. These plants were self-pollinated, and the progeny were used to positionally clone *qSOR1*.

Vector Construction and Rice Transformation. For the complementation tests (gSA), BACs of SA (SA08M07) and GB (GB36P04) were each selected from the corresponding BAC libraries that were constructed as described previously (52). A 7.57-kb genomic fragment of SA containing the *qSOR1* region was excised from the BAC clone SA08M07 by ApaI and XbaI, and then cloned into the pPZP2H-lac binary vector (53). For genome editing, the CRISPR/*Cas9* cleavage sites of *qSOR1*, *DRO1*, and *DRL2*, were designed using CRISPRdirect (https://crispr.dbcls.jp), and the vectors were constructed using a previously published method (54). We then cloned the gRNA expression cassettes into the pZDgRNA binary vector by AscI and PacI. The primers used in this experiment are shown in the *SI Appendix*, Table S4. All generated constructs were introduced into the *Agrobacterium tumefaciens* strain EHA105 by electroporation. *Agrobacterium*-mediated transformation of the rice was then performed as described previously (55). Control plants were generated by introducing the empty binary vectors. Single-copy selection was conducted using the hygromycin phosphotransferase gene.

RNA Isolation and Expression Analysis by qRT-PCR. Total RNA was isolated from various tissues, using the RNeasy Plant Mini Kit (Qiagen), according to the manufacturer's instructions. First-strand cDNA was synthesized using SuperScript II reverse transcriptase (Invitrogen). qRT-PCR using TaqMan probes was performed using specific primers and probes that are listed in *SI Appendix*, Table S4. PCR conditions were: 30 s at 95 °C followed by 40 cycles of 15 s at 95 °C and 1 min at 60 °C. Expression of the target genes was normalized to a ubiquitin gene. To examine the effects of the exogenous auxin treatments, seedlings were soaked in water containing 10 μM 2,4-dichlorophenoxyacetic acid for designated lengths of time. For the inhibition of protein synthesis, seedlings were soaked in water containing 100 μM CHX (Wako) or DMSO (control) for 1 h as a pretreatment, and then 2,4-dichlorophenoxyacetic acid was diluted with growth media to 10 μM (DMSO for control) and incubated for 3 h.

In Situ Hybridization. To investigate the spatial expression patterns of *qSOR1*, we collected root tips (3–4 mm in length) from 2-d-old SA, qsor1-NIL, and GB plants grown on 0.4% agarose (Sigma). To investigate *qSOR1* expression in the root tips after rotation, we collected the root tips (3–4 mm in length) after rotations of 90° from the original vertical axis for 1.5 h, using 2-d-old seedlings grown on 0.4% agarose. Tissue fixation, hybridization, and immunological detection of the hybridized probes were performed as described previously (56), with minor modifications. For the probes, amplified *qSOR1* fragments were subcloned into pBluescript II KS+ (Stratagene). Digoxigenin-labeled antisense and sense probes were transcribed using a MAXIscript T7 In Vitro Transcription Kit (Ambion).

Evaluation of Root Gravitropic Curvature. We measured root gravitropic curvature of the seedlings in the SA, qsor1-NIL, and transgenic plants after rotating the roots from the normal vertical axis to the horizontal axis for 4 h, as described previously (16). Seedlings were grown for 36–48 h on 0.4% agarose, in the dark at 28 or 30 °C. For evaluation of the root gravitropic responses under salt stress, we measured the root gravitropic curvature of the seedlings in SA, qsor1-NIL, [*DRO1*, *qSOR1*], [*DRO1*, *qsor1*], [*dro1*, *qSOR1*], and [*dro1*, *qsor1*] plants. In normal culture conditions, the seedlings were grown for 1 d on 0.4% agarose in the dark at 30 °C and were then rotated. For the salt stress conditions, the seedlings were grown on 0.4% agarose with 50 mM NaCl. The root curvature was measured at the specified time intervals after rotation. The data from each rotation angle was averaged for each line. Root curvature was measured using ImageJ (rsbweb.nih.gov/ij/).

Measurement of Columella Cell Size. To observe the amyloplasts in the columella cells, we collected root tips (3–4 mm in length) from 1-d-old seedlings of SA, qsor1-NIL, [*DRO1*, *qSOR1*], [*DRO1*, *qsor1*], [*dro1*, *qSOR1*], and [*dro1*, *qsor1*] plants grown on 0.4% agarose in the dark at 30 °C. The root tips were stained with I_2-KI solution for 1 min. The stained roots were then spread on a microscope slide and mounted either with chloral hydrate solution (8 g of chloral hydrate, 2 mL of water, 1 mL of glycerol). The root tips were observed under a light microscope (AX70, Olympus). To measure the columella cell sizes, we collected the crown root tips (3–4 mm in length) from 1-mo-old plants of the six lines grown in stainless-steel mesh baskets. After tissue fixation with formalin–acetic acid–alcohol, 8-μm-thick paraffin sections of each line were made and stained with hematoxylin. The longitudinal length and width of the columella were measured using ImageJ. The length of the columella cells was calculated by dividing the total length of the columella by the number of columella cells.

Sequence Alignment and Phylogenetic Tree Construction. BLAST searches were performed using the amino acid sequences of DRO1 or qSOR1 as queries, and the protein sequences used to construct the phylogenetic trees can be found in the UniProtKB (https://www.uniprot.org/) database. The tree was constructed using a maximum likelihood algorithm with MEGA X (57). Full-length amino acid sequences were aligned by ClustalW to build the tree.

Subcellular Localization Analysis. The ORF sequences of *qSOR1* and *qsor1* were amplified by PCR with cDNA as the template, using specific primers (*SI Appendix*, Table S4). The fragments were subcloned into pENTER4 (Invitrogen) with the in-fusion directional cloning kit (Takara). The verified plasmids

were mixed with the destination vector pSAT6-DEST-EGFP-N1 (58) by Gateway LR Clonase (Invitrogen). Then, 2 × 35Sprom::qSOR1(sa)-EGFP, 2 × 35Sprom::qSOR1(gb)-EGFP, 2 × 35Sprom::EGFP, and the plasma membrane marker UBQ10prom::2×CHERRY-1×PH^{OSBP} (59) were transfected to the protoplasts of young rice seedlings, using a previously described method, with a slight modification (60, 61). Briefly, rice stems of 1-wk-old seedlings were cut into 1-cm segments with a razor blade and then digested with cellulase solution including 10 mM β-mercaptoethanol. The protoplast suspension was prepared as described previously (61), and then 40 μL of protoplast suspension (ca. 1,000 cells) was transfected with 1 μg of DNA for these constructs into a 96-well plate. The EGFP and mCherry fluorescence was observed with a TCS SP5 confocal laser scanning microscope (Leica), according to the manufacture's protocol, after incubation overnight.

Quantification of Vertical Root Distribution. We investigated the vertical root distributions of IR64 and its three introgression lines using the trench method, as described previously (16). Plants were grown in an upland field under well-watered conditions at NARO (36°03′N, 140°10′E) in Tsukuba, Japan, in the summer of 2016. One hundred days after sowing, the soil was dug up near the hills of the plants and their root zones were observed. To quantify the root distributions of the rice plants, we took soil monoliths (30 × 30 × 5 cm) from the root area of the 97-d-old plants, using a metal monolith sampler and following the soil monolith method, as described previously (16). Samples were taken from the same field in which we used the trench method before conducting soil excavations. Each soil monolith was divided into 12 blocks, as illustrated in Fig. 3C. The roots in each block were washed, oven dried at 80 °C for 3 d, and then weighed to obtain the root dry weight.

Evaluation of Yield Performance under Salinity Stress Conditions. We investigated the grain yields of SA and the qsor1-NIL in the experimental paddy fields irrigated with fresh (control) and saline water from 2015 to 2018. Field experiments were conducted at the Experimental Farm Station (38°47′N, 141°06′E), Graduate School of Life Sciences, Tohoku University, in Kashimadai, Osaki, Miyagi prefecture, Japan, as described previously (62). Forty-nine seedlings were transplanted to 2.1 × 2.1 m research plots in the paddy fields, with at least three replications, in late May. The space between the hills was 30 cm. Four weeks after transplantation, the saline plots were flooded with saline water (Salt; 1.0–1.2%), whereas the control plots were continuously supplied with fresh water (salt; less than 0.01%). In the saline plots, the salt concentration of the paddy water was maintained at about 0.4% by flooding with saline or fresh water once a week. The salt concentrations in the floodwater were determined using a portable salt meter (APAL-ES1, AZ-ONE). To measure the salt concentrations in the soil with saline or fresh water, undisturbed soil columns were sampled from the lower cultivated soil layers (depth 5–10 cm), using a stainless-steel tube (5 cm diameter × 5 cm height), in 2016. Pore water from the soil columns was collected using a high-pressure centrifugal displacement method with a soil dehydration rotor (RPRD11, Koki Holdings) and the EC (electric conductivity) values were measured, equivalent to those at the standard 25 °C, using a conductivity electrode. For example, EC at a salt concentration of 0.4% is 7.5 dS·m^{-1} at 25 °C. We evaluated the soil-surface rooting of the nine plants for each plot in the paddy field, using the basket method, as described previously (20). Around 45–60 d after transplanting,

we dug out baskets and counted the number of primary roots growing over the opensides of the baskets. During the harvest in late September, 25 plants were sampled, avoiding the border areas of the plots. After harvesting, each plant was dried and divided into panicle and stem parts to measure the dry weights of each part. Husks of the grains were removed with an experimental rice-hulling machine, and the weight of the brown rice grains was measured. The brown rice grains were classified by sifting them through different sizes of mesh in an electric sieve.

To quantify the sodium ions in the xylem exudates, we collected the xylem exudates from the rice plants approximately 2 wk after heading in 2018. To obtain the exudates, the shoots were cut 15 cm above the soil surface, and a plastic wrap containing cotton wool was attached to each cut end of the basal shoot part with a rubber band. The cotton, including the exudates, was detached 2 h later and weighed. After adding extrapure water to the cotton with the exudates, the samples were extracted with ultrasonic waves and diluted in a 0.1 M nitric acid aqueous solution. The amount of Na$^+$ in the extract was quantified by atomic absorption spectrophotometry (Z-5010, Hitachi). Three individuals were collected as one bulk sample. Two bulk samples from two plots of each treatment were obtained, creating a total of four bulk samples from each treatment.

Before plowing, the bulk soils were collected from the saline and normal paddy fields in 2018 and 2019. These bulk soils were air-dried and sieved through a 1 cm-mesh. These soil samples were used to fill plastic pots, and then these pots were filled with saline (salt concentration; 0.4%) or tap water. The soil samples were mixed with a stirring tool, to promote the absorption of the water in the pots, and they were watered with tap water every 2 to 3 d to maintain a constant water level in the greenhouse. The oxidation-reduction potential (ORP) at a 5-cm depth in the soil was measured with ORP Electrodes (9300-10D, HORIBA).

Statistical Methods. All statistical analyses were performed with JMP v. 11.2.1 software (SAS Institute).

Data Availability. The data supporting the findings of the study and associated protocols are available in this article and its *SI Appendix*. Plant materials used in this study are available upon request to the corresponding author. The DNA Data Bank of Japan (DDBJ) accessions for *qSOR1* from SA and GB are LC494454 and LC494455, respectively.

1. S. Roychoudhry, S. Kepinski, Shoot and root branch growth angle control-the wonderfulness of lateralness. *Curr. Opin. Plant Biol.* **23**, 124–131 (2015).
2. G. T. Freschet, E. Kichenin, D. A. Wardle, Explaining within-community variation in plant biomass allocation: A balance between organ biomass and morphology above vs below ground? *J. Veg. Sci.* **26**, 431–440 (2015).
3. P. Hedden, The genes of the green revolution. *Trends Genet.* **19**, 5–9 (2003).
4. B. Yu et al., TAC1, a major quantitative trait locus controlling tiller angle in rice. *Plant J.* **52**, 891–898 (2007).
5. Y. Jiao et al., Regulation of OsSPL14 by OsmiR156 defines ideal plant architecture in rice. *Nat. Genet.* **42**, 541–544 (2010).
6. K. Miura et al., OsSPL14 promotes panicle branching and higher grain productivity in rice. *Nat. Genet.* **42**, 545–549 (2010).
7. J. P. Lynch, K. M. Brown, Topsoil foraging–An architectural adaptation of plants to low phosphorus availability. *Plant Soil* **237**, 225–237 (2001).
8. Y. Uga, Y. Kitomi, S. Ishikawa, M. Yano, Genetic improvement for root growth angle to enhance crop production. *Breed. Sci.* **65**, 111–119 (2015).
9. Y. Mano, F. Omori, Breeding for flooding tolerant maize using "teosinte" as a germplasm resource. *Plant Root* **1**, 17–21 (2007).
10. E. D. Rogers, P. N. Benfey, Regulation of plant root system architecture: Implications for crop advancement. *Curr. Opin. Biotechnol.* **32**, 93–98 (2015).
11. Y. Kitomi, J. Itoh, Y. Uga, "Genetic mechanisms involved in the formation of root system architecture" in *Rice Genomics, Genetics and Breeding*, T. Sasaki, M. Ashikari, Eds. (Springer Nature, Singapore, 2018), pp. 243–274.
12. L. Wang et al., *LARGE ROOT ANGLE1*, encoding OsPIN2, is involved in root system architecture in rice. *J. Exp. Bot.* **69**, 385–397 (2018).
13. M. Bettembourg et al., Root cone angle is enlarged in docs1 LRR-RLK mutants in rice. *Rice (N. Y.)* **10**, 50 (2017).
14. G. Huang et al., Rice actin binding protein RMD controls crown root angle in response to external phosphate. *Nat. Commun.* **9**, 2346 (2018).
15. M. V. Mickelbart, P. M. Hasegawa, J. Bailey-Serres, Genetic mechanisms of abiotic stress tolerance that translate to crop yield stability. *Nat. Rev. Genet.* **16**, 237–251 (2015).
16. Y. Uga et al., Control of root system architecture by *DEEPER ROOTING 1* increases rice yield under drought conditions. *Nat. Genet.* **45**, 1097–1102 (2013).
17. K. Ueno, T. Sato, Aerial root formation in rice ecotype Bulu. *Jpn. J. Trop. Agr.* **33**, 173–175 (1989).
18. H. R. Lafitte, M. C. Champoux, G. McLaren, J. C. O'Toole, Rice root morphological traits are related to isozyme group and adaptation. *Field Crops Res.* **71**, 57–70 (2001).
19. Y. Uga et al., Identification of qSOR1, a major rice QTL involved in soil-surface rooting in paddy fields. *Theor. Appl. Genet.* **124**, 75–86 (2012).
20. E. Hanzawa et al., Isolation of a novel mutant gene for soil-surface rooting in rice (Oryza sativa L.). *Rice (N. Y.)* **6**, 30 (2013).
21. T. Sakai et al., The wavy growth 3 E3 ligase family controls the gravitropic response in Arabidopsis roots. *Plant J.* **70**, 303–314 (2012).
22. H. Chen et al., E3 ubiquitin ligase SOR1 regulates ethylene response in rice root by modulating stability of Aux/IAA protein. *Proc. Natl. Acad. Sci. U.S.A.* **115**, 4513–4518 (2018).

AGRICULTURAL SCIENCES

23. F. D. Sack, Plant gravity sensing. *Int. Rev. Cytol.* **127**, 193–252 (1991).
24. T. Ulmasov, G. Hagen, T. J. Guilfoyle, ARF1, a transcription factor that binds to auxin response elements. *Science* **276**, 1865–1868 (1997).
25. G. Hagen, T. Guilfoyle, Auxin-responsive gene expression: Genes, promoters and regulatory factors. *Plant Mol. Biol.* **49**, 373–385 (2002).
26. T. Yoshihara, E. P. Spalding, M. Iino, AtLAZY1 is a signaling component required for gravitropism of the *Arabidopsis thaliana* inflorescence. *Plant J.* **74**, 267–279 (2013).
27. L. Ge, R. Chen, Negative gravitropism in plant roots. *Nat. Plants* **2**, 16155 (2016).
28. J. M. Guseman, K. Webb, C. Srinivasan, C. Dardick, *DRO1* influences root system architecture in Arabidopsis and Prunus species. *Plant J.* **89**, 1093–1105 (2017).
29. M. Taniguchi *et al.*, The Arabidopsis LAZY1 family plays a key role in gravity signaling within statocytes and in branch angle control of roots and shoots. *Plant Cell* **29**, 1984–1999 (2017).
30. Y. Kitomi *et al.*, QTLs underlying natural variation of root growth angle among rice cultivars with the same functional allele of *DEEPER ROOTING 1*. *Rice (N. Y.)* **8**, 16 (2015).
31. A. Ashraf *et al.*, Evolution of *Deeper Rooting 1-like* homoeologs in wheat entails the C-terminus mutations as well as gain and loss of auxin response elements. *PLoS One* **14**, e0214145 (2019).
32. M. Furutani *et al.*, Polar recruitment of RLD by LAZY1-like protein during gravity signaling in root branch angle control. *Nat. Commun.* **11**, 76 (2020).
33. P. Li *et al.*, *LAZY1* controls rice shoot gravitropism through regulating polar auxin transport. *Cell Res.* **17**, 402–410 (2007).
34. F. Sun *et al.*, Salt modulates gravity signaling pathway to regulate growth direction of primary roots in Arabidopsis. *Plant Physiol.* **146**, 178–188 (2008).
35. Y. Mano, F. Omori, M. Muraki, T. Takamizo, QTL mapping of adventitious root formation under flooding conditions in tropical maize (*Zea mays* L.) seedlings. *Breed. Sci.* **55**, 343–347 (2005).
36. Y. Mano, F. Omori, C. H. Loaisiga, R. M. Bird, QTL mapping of above-ground adventitious roots during flooding in maize x teosinte "*Zea nicaraguensis*" backcross population. *Plant Root* **3**, 3–9 (2009).
37. M. Nakamura, T. Nishimura, M. T. Morita, Bridging the gap between amyloplasts and directional auxin transport in plant gravitropism. *Curr. Opin. Plant Biol.* **52**, 54–60 (2019).
38. M. Qadir, S. Schubert, Degradation processes and nutrient constraints in sodic soils. *Land Degrad. Dev.* **13**, 275–294 (2002).
39. P. K. Srivastava *et al.*, Effects of sodicity induced changes in soil physical properties on paddy root growth. *Plant Soil Environ.* **60**, 165–169 (2014).
40. G. B. Gregorio *et al.*, Progress in breeding for salinity tolerance and associated abiotic stresses in rice. *Field Crops Res.* **76**, 91–101 (2002).
41. W. Armstrong, S. H. F. W. Justin, P. M. Beckett, S. Lythe, Root adaptation to soil waterlogging. *Aquat. Bot.* **39**, 57–73 (1991).
42. Y. Mano, F. Omori, H. Tamaki, S. Mitsuhashi, W. Takahashi, DNA marker-assisted selection approach for developing flooding-tolerant Maize. *Jpn. Agric. Res. Q.* **50**, 175–182 (2016).
43. H. Ye *et al.*, A major natural genetic variation associated with root system architecture and plasticity improves waterlogging tolerance and yield in soybean. *Plant Cell Environ.* **41**, 2169–2182 (2018).
44. Y. Takai, T. Kamura, The mechanism of reduction in waterlogged paddy soil. *Folia Microbiol. (Praha)* **11**, 304–313 (1966).
45. N. K. Fageria, A. B. Santos, M. P. Barbosa Filho, C. M. Guimarães, Iron toxicity in lowland rice. *J. Plant Nutr.* **31**, 1676–1697 (2008).
46. S. Waidmann *et al.*, Cytokinin functions as an asymmetric and anti-gravitropic signal in lateral roots. *Nat. Commun.* **10**, 3540 (2019).
47. K. Butcher, A. F. Wick, T. DeSutter, A. Chatterjee, J. Harmon, Soil salinity: A threat to global food security. *Agron. J.* **108**, 2189–2200 (2016).
48. T. Gopalakrishnan, M. D. Hasan, A. T. M. S. Haque, S. L. Jayasinghe, L. Kumar, Sustainability of coastal agriculture under climate change. *Sustainability* **11**, 7200 (2019).
49. L. Ku *et al.*, Cloning and characterization of a putative TAC1 ortholog associated with leaf angle in maize (*Zea mays* L.). *PLoS One* **6**, e20621 (2011).
50. C. Dardick *et al.*, PpeTAC1 promotes the horizontal growth of branches in peach trees and is a member of a functionally conserved gene family found in diverse plants species. *Plant J.* **75**, 618–630 (2013).
51. Y. Uga, K. Okuno, M. Yano, Fine mapping of *Sta1*, a quantitative trait locus determining stele transversal area, on rice chromosome 9. *Mol. Breed.* **26**, 533–538 (2010).
52. Y. Hattori *et al.*, The ethylene response factors *SNORKEL1* and *SNORKEL2* allow rice to adapt to deep water. *Nature* **460**, 1026–1030 (2009).
53. T. Fuse, T. Sasaki, M. Yano, Ti-plasmid vectors useful for functional analysis of rice genes. *Plant Biotechnol.* **18**, 219–222 (2001).
54. M. Mikami, S. Toki, M. Endo, Comparison of CRISPR/Cas9 expression constructs for efficient targeted mutagenesis in rice. *Plant Mol. Biol.* **88**, 561–572 (2015).
55. Y. Hiei, S. Ohta, T. Komari, T. Kumashiro, Efficient transformation of rice (*Oryza sativa* L.) mediated by Agrobacterium and sequence analysis of the boundaries of the T-DNA. *Plant J.* **6**, 271–282 (1994).
56. T. Komatsuda *et al.*, Six-rowed barley originated from a mutation in a homeodomain-leucine zipper I-class homeobox gene. *Proc. Natl. Acad. Sci. U.S.A.* **104**, 1424–1429 (2007).
57. S. Kumar, G. Stecher, M. Li, C. Knyaz, K. Tamura, MEGA X: Molecular evolutionary genetics analysis across computing platforms. *Mol. Biol. Evol.* **35**, 1547–1549 (2018).
58. T. Tzfira *et al.*, pSAT vectors: a modular series of plasmids for autofluorescent protein tagging and expression of multiple genes in plants. *Plant Mol. Biol.* **57**, 503–516 (2005).
59. M. L. A. Simon *et al.*, A multi-colour/multi-affinity marker set to visualize phosphoinositide dynamics in Arabidopsis. *Plant J.* **77**, 322–337 (2014).
60. Y. Fujikawa *et al.*, Split luciferase complementation assay to detect regulated protein-protein interactions in rice protoplasts in a large-scale format. *Rice (N. Y.)* **7**, 11 (2014).
61. S. Sakamoto, K. Matsui, Y. Oshima, N. Mitsuda, Efficient transient gene expression system using buckwheat hypocotyl protoplasts for large-scale experiments. *Breed. Sci.* **70**, 128–134 (2020).
62. H. Takehisa *et al.*, Epistatic interaction of QTLs controlling leaf bronzing in rice (*Oryza sativa* L.) grown in a saline paddy field. *Breed. Sci.* **56**, 287–293 (2006).